Robotica (2008) volume 26, pp. 395–403. © 2008 Cambridge University Press
doi:10.1017/S0263574707004109 Printed in the United Kingdom

Workspaces associated to assembly modes of the 5R planar parallel manipulator

Erik Macho, Oscar Altuzarra, Charles Pinto and Alfonso Hernandez*

Department of Mechanical Engineering, University of the Basque Country, Bilbao, 48013, Spain

(Received in Final Form: December 17, 2007. First published online: February 1, 2008)

SUMMARY
The aim of this paper is to show how it is possible to obtain for the 5R planar parallel manipulator the complete workspace associated with each solution of the direct kinematic problem or assembly mode. The workspaces associated with the different inverse kinematic problem solutions or working modes are joined and the robot moves from one to another without losing the control. An exhaustive analysis of the complete workspace and singular positions of the 5R planar parallel manipulator with two active joints is presented. Furthermore, application of these principles to path planning will be explained.

KEYWORDS: Parallel manipulator; Working modes; Assembly modes; Singularities; Workspace; Path planning; 5R manipulator.

1. Introduction
Parallel manipulators are an interesting alternative to serial manipulators given the important mechanical and kinematic advantages offered, i.e., better stiffness and payload, higher natural frequencies and accuracy, more convenient location of the actuators, higher velocity and acceleration of the end-effector, etc.[1] Nevertheless, in counterpart they often present more limited and complex workspaces with internal singularities.[2–4] Thus, the workspace size, shape and quality are considered the main design criteria of these robots.[5]

The fact that these mechanisms generally present multiple solutions for both direct and inverse kinematic problems has been for a long time a research topic. A common practice in the use of these manipulators is to keep at all times the same solution for both direct and inverse problems. On the one hand, there are constructive problems which can justify this. On the other hand, it was commonly thought that to perform a transition between solutions, the robot must go through a singularity pose where it becomes uncontrollable.[6]

Recent applications are trying to show the practicability of changing between different kinematic solutions, whereby the workspaces associated with each solution may be joined to form a larger practical workspace.[7] Nevertheless, in this approach singularity poses are crossed making use of the gravity effect, which may imply a certain risk of uncontrollability.

On the contrary, some authors have managed to prove that it is possible to join different direct kinematic problem solutions via paths totally free of singularities.[8,9,10]

The 5R planar parallel manipulator is a well-known mechanism whose characteristics have been studied by different researchers, e.g., its kinematics in ref. [11] focused on the symmetrical manipulator, or in ref. [12], focused on the inverse kinematic problem resolution; its singularities in ref. [13] obtained in the joint space, or in ref. [14] applicable to manipulators using differential gear drives; its workspace in ref. [15] one of the pioneering works, or in ref. [16] for the 5R as part of an hybrid manipulator; and some performance atlases in ref. [17, 18] where conditioning indices are obtained in the solution space.

In recent works about the 5R,[19,20] internal singularity-free workspaces corresponding to the different working modes and assembly modes are obtained. But they suggest that the mechanism should never change its configuration, neither the assembly mode nor the working mode. Furthermore no mention is made of the possibility of changing the working mode. Other works related to the 5R workspace and singularities propose how to obtain the entire workspace associated with an assembly mode.[21,22] However, they do not explain how to do the path planning to change the working mode without reaching a singular posture.

This paper emphasises the possibility of enlarging the workspace by joining the different inverse kinematic problem solutions, maintaining the same direct kinematic problem solution. To illustrate the entire process the 5R planar parallel manipulator will be used, since its workspace admits a complete representation on the plane. But this application could be considered as the particularisation of a more general methodology. This paper aims to complete the 5R planar manipulator study with a view to do a really effective path planning.

2. The 5R Planar Manipulator
The 5R planar parallel manipulator is a two degrees of freedom mechanism. As shown in Fig. 1, the actuators are located in the fixed revolute joints, A_1 and A_2, so the input variables are θ_1 and θ_2 angles. The output variables are x and y coordinates of point P. Revolute joints B_1, B_2 and P are passive kinematic pairs.

Without loss of generality, the figures appearing in this work refer to a manipulator with the following dimensions. An asymmetrical manipulator has been selected in order to

* Corresponding author. E-mail: a.hernandez@ehu.es

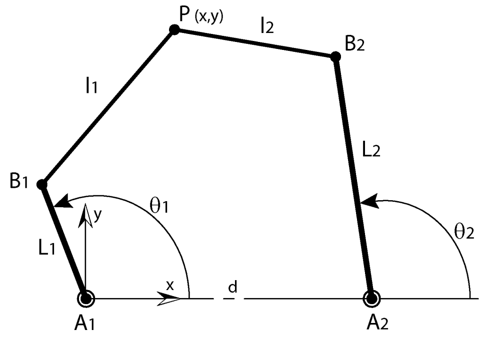

Fig. 1. 5R Planar manipulator notation.

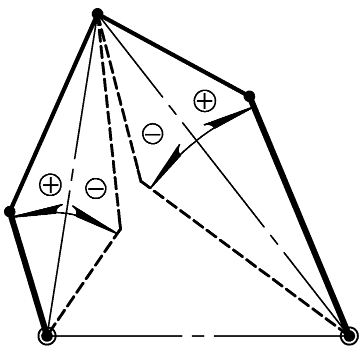

Fig. 2. IKP solutions. Working modes.

analyse a general case.

$$L_1 = 15, \quad L_2 = 30$$
$$l_1 = 25, \quad l_2 = 20$$
$$d = 35$$

2.1. *Working modes*

The inverse kinematic problem (IKP) consists in obtaining the values of the input variables when the output variables are given.

In this case, as indicated in Fig. 2, given the x and y coordinates of P, each of the kinematic chains reaching that point may represent two different solutions, so two possible values of each angle θ_i are possible.

The distinctive symbols of each possible configuration of each chain are differentiated in Fig. 2. As there are two kinematic chains, each with two possible configurations, the mechanism presents four possible working modes altogether, namely $\oplus\oplus$, $\ominus\ominus$, $\oplus\ominus$ and $\ominus\oplus$.

2.2. *Assembly modes*

Given the values of the input variables, θ_1 and θ_2, two different positions of point P, i.e., two solutions of the direct kinematic problem (DKP), can be obtained and correspond to the two assembly modes. In Fig. 3 are indicated the distinctive symbols, $\oplus$ and $\ominus$, for each of the two possible configurations. These symbols are coincident with the sign of the angles α_i.

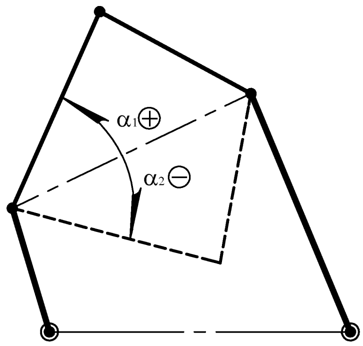

Fig. 3. DKP solutions. Assembly modes.

2.3. *Singularity analysis*

The velocity problem can be expressed in matrix form as

$$\mathbf{A}\begin{Bmatrix}\dot{x}\\ \dot{y}\end{Bmatrix} = \mathbf{B}\begin{Bmatrix}\dot{\theta}_1\\ \dot{\theta}_2\end{Bmatrix} \tag{1}$$

where

$$\mathbf{A} = \begin{bmatrix}\mathbf{l}_1^T\\ \mathbf{l}_2^T\end{bmatrix} \tag{2}$$

$$\mathbf{B} = \begin{bmatrix}(\mathbf{L}_1 \times \mathbf{l}_1)^T\\ (\mathbf{L}_2 \times \mathbf{l}_2)^T\end{bmatrix} \tag{3}$$

being

$$\mathbf{L}_i = \begin{Bmatrix}B_i^x - A_i^x\\ B_i^y - A_i^y\end{Bmatrix}, \quad \mathbf{l}_i = \begin{Bmatrix}P^x - B_i^x\\ P^y - B_i^y\end{Bmatrix} \tag{4}$$

2.3.1. *Type I singularities.*

Type I singularities are the singular solutions of the IKP. They arise when matrix $\mathbf{B}$ becomes singular,[2] which happens when $\mathbf{L}_1$ is parallel to $\mathbf{l}_1$ or when $\mathbf{L}_2$ is parallel to $\mathbf{l}_2$. These singularities determine the workspace boundaries as shown in Fig. 4. In these positions a linear dependence ratio is verified between the output velocities $\dot{x}$ and $\dot{y}$.

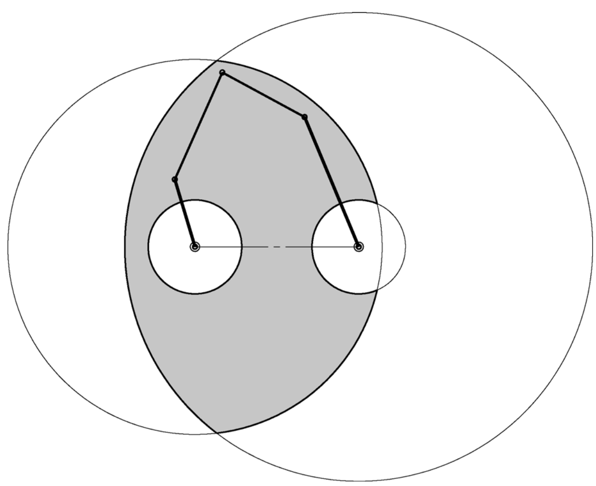

Fig. 4. Type I singularity loci and workspace.

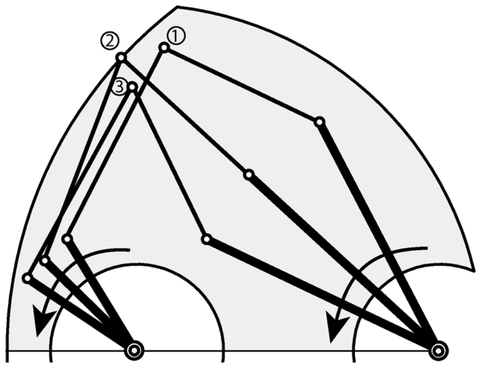

Fig. 5. Crossing a type I singularity.

The IKP singularity loci is given by the following equations:

$$x^2 + y^2 = (L_1 \pm l_1)^2 \tag{5}$$

$$(x-d)^2 + y^2 = (L_2 \pm l_2)^2 \tag{6}$$

Any transition from one working mode to another necessarily implies that point P follows a path passing through one of these curves. It is important to emphasise that at the workspace boundary, these transitional postures may be considered inappropriate at an operational level due to manipulability restrictions, but they do not imply a loss of control. Such a transition can be seen in Fig. 5, where the mechanism is initially located in the $\oplus\oplus$ working mode (position 1) and moves to the $\oplus\ominus$ working mode (position 3) passing through a type I singularity (position 2).

2.3.2. Type II singularities. Type II singularities are DKP singular solutions and they arise when matrix $\mathbf{A}$ becomes singular, which occurs when $\boldsymbol{l}_1$ and $\boldsymbol{l}_2$ are collinear. In this case a linear dependence ratio appears between input velocities $\dot{\theta}_1$ and $\dot{\theta}_2$.

Type II singularities may be obtained computing the paths of point P, considered as the end-effector of the 4R mechanism that results from the alignment of bars l_1 and l_2, at 0 or at 180, as shown in Fig. 6.

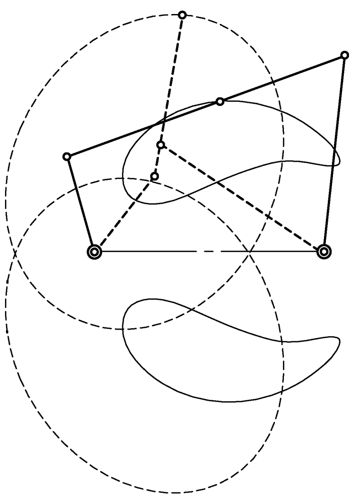

Fig. 6. Type II singularity loci.

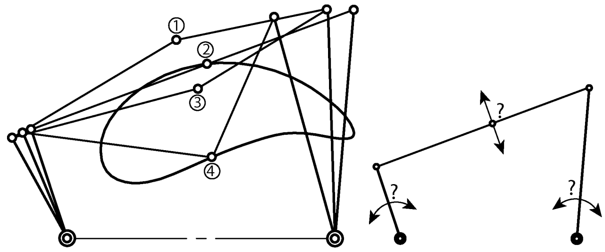

Fig. 7. Passing through a type II singularity.

Therefore, DKP singularity loci is given by the following equations (in the Roberts form):

$$U^2 + V^2 = W^2 \tag{7}$$

where

$$U = l_1 x\left((x-d)^2 + y^2 + l_2^2 - L_2^2\right) - l_2\left(y\sin\alpha + (x-d)\cos\alpha\right)\left(x^2 + y^2 + l_1^2 - L_1^2\right) \tag{8}$$

$$V = l_2(y\cos\alpha - (x-d)\sin\alpha)\left(x^2 + y^2 + l_1^2 - L_1^2\right) - l_1 y\left((x-d)^2 + y^2 + l_2^2 - L_2^2\right) \tag{9}$$

$$W = 2l_1 l_2(\mathrm{d}y\cos\alpha - (x(x-d) + y^2)\sin\alpha) \tag{10}$$

being the value of α either 0 (closed 4R, dashed line in Fig. 6), or π (open 4R, continuous line).

Going from one assembly mode to the other one necessarily means that point P reaches one of these singularity curves. In Fig. 7 the mechanism is initially located in the $\oplus$ assembly mode (position 1). To reach the $\ominus$ assembly mode (position 3), point P must pass necessarily through a DKP singularity (position 2). An undesirable loss of control occurs in this DKP singular posture.

2.3.3. Increased mobility singularities. Another singularity type may appear in parallel manipulators different from type I and type II singularities. These are the increased mobility singularities,[3] which appear when the mechanism presents an increase in its instantaneous mobility. Thus, additional inputs are required to define the motion in such positions. In the 5R case, these singularities could only appear in positions where the five bars were aligned. In the proposed example this is not possible since the mechanism needs to verify certain ratios among the dimensions of its elements to satisfy that condition.

2.3.4. Tangency points between type I and type II singularity loci. There are certain positions that simultaneously verify type I and type II singularities, i.e., positions where the Jacobian matrices $\mathbf{A}$ and $\mathbf{B}$ become both singular at the same time. This does not mean that the mechanism will present a different behaviour; therefore, these points do not imply a new kind of singularity. Figure 8 shows the previously obtained DKP and IKP singularity loci superimposed, verifying a series of tangency points, t_i, among them. These points, common to both curve types, represent positions where combined singularities occur. They are positions where bars l_1, l_2 and L_1 or bars l_1, l_2 and L_2 are aligned.

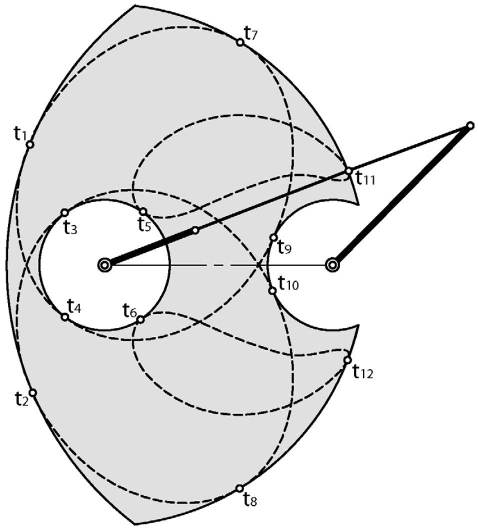

Fig. 8. Tangency points between the direct and inverse singularity locies.

The number of these tangency points in a 5R manipulator is always even. Depending on the mechanism dimensions these may vary up to a maximum of 16. In this case there are 12.

3. Type II Singularities Associated with Working Modes

Figure 8 shows the manipulator complete workspace, whose boundaries are given by type I singularity curves, containing the type II singularity curves inside. Whenever point *P* reaches a workspace boundary, the mechanism is within a type I singularity. However, it should be emphasised that although *P* reaches a position on one of the type II singularity curves, it is not always a true singularity position, e.g., position 4 in Fig. 7. This is due to the association between type II singularities and working modes.

Type II singularity loci results in some closed curves. However, the aforementioned tangency points divide these closed curves on a series of open curves. Each of those open curves between tangent points will represent type II singularities for one working mode, but ordinary positions for the rest. Thus, by identifying each open curve it will be possible to distribute the entire set of type II singularities among the four working modes.

In Fig. 9, true type II singularities for each working mode are represented by dashed lines. In addition, it is shown that all the working modes present the same type I singularity loci (same workspace boundary). Furthermore, the symbols ⊕ and ⊖ have been used in this figure to indicate which assembly mode corresponds to each region of the workspace.

4. Workspace Regions

Let us place the mechanism in an initial position with ⊕⊕ working mode and ⊕ assembly mode as shown in Fig. 9(a). The type II singularity curves divide the workspace into a series of adjacent regions. Each of these regions is free of any kind of internal singularity since its boundaries are made up of singularity curves. Each region is separated

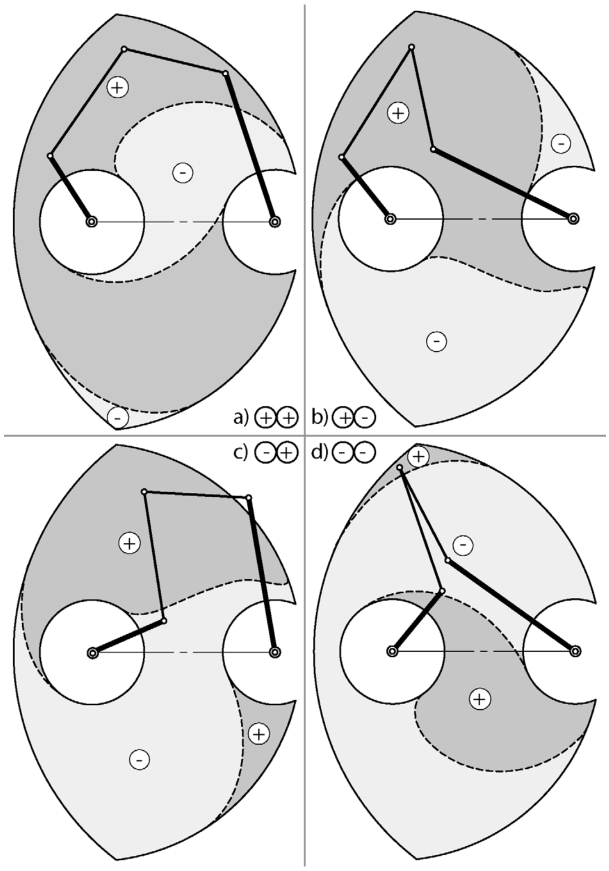

Fig. 9. Type II singularities associated with different working modes.

from the adjacents by type II singularities. Two adjacent regions will always correspond to different assembly modes, i.e., ⊕ on one side and ⊖ on the other, because a type II singularity curve separates positions where the assembly mode is inverted.

If the manipulator is situated in an initial position like the one described above, the workspace region where it is located can be identified immediately and is illustrated in Fig. 10(a).

In Fig. 10 it can be checked how each region is delimited by two types of curves, those corresponding to type I singularities (continuous line) and those corresponding to type II singularities (dashed line). As mentioned above, type II singularities imply loss of mechanism control or manipulability and hence these positions should be considered forbidden for all effects. Nevertheless, type I singularities, although being positions where operability is constrained, do not represent a problem from the actuators' control point of view.

5. Relations Among Workspace Regions

In order to illustrate this, let us start from the initial position indicated in Fig. 10(a) and perform a change of working mode from ⊕⊕ to ⊕⊖, with the final position as in Fig. 10(b), through a type I singularity. Immediately after reaching the workspace boundary, the mechanism can move to the new working mode, where as established, type II singularities are not the same as those in the starting position. Thus, in this new situation the workspace is divided into regions different

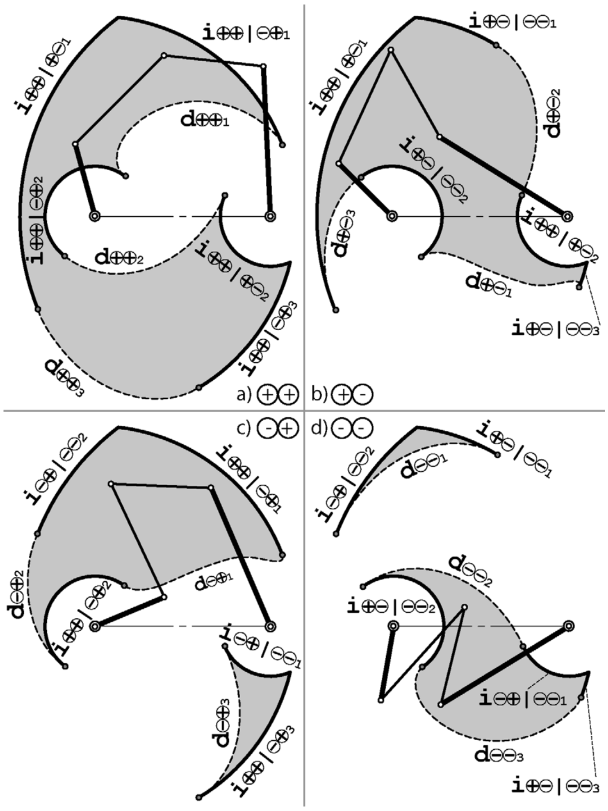

Fig. 10. Regions corresponding to ⊕ assembly mode in the four working modes.

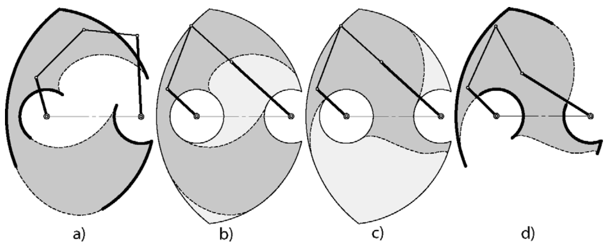

Fig. 11. Change of working mode.

from the previous ones. The process described is illustrated in Fig. 11.

A relevant fact to be emphasised is that during the transition between the working modes, a type II singularity has at no time been reached. Thus the assembly mode before and after the inverse configuration change is ⊕.

In Fig. 12 the workspace regions where point P is found before and after the working mode change are represented superimposed, enabling a series of remarks. First, it is checked that new positions which were not feasible before can now be reached by the manipulator. Second, it is shown that both regions have some common boundaries represented by the dashed lines. These curves constitute precisely the gates allowing transition from one working mode to the other. Physically those gates are the type I singularities generated by the kinematic chain which changes its configuration. All the gates whereby it is possible to make working mode changes are identified in Fig. 10 as i⊕ ⊕ ∥ ⊕ ⊖, indicating the two regions between which the change is enabled.

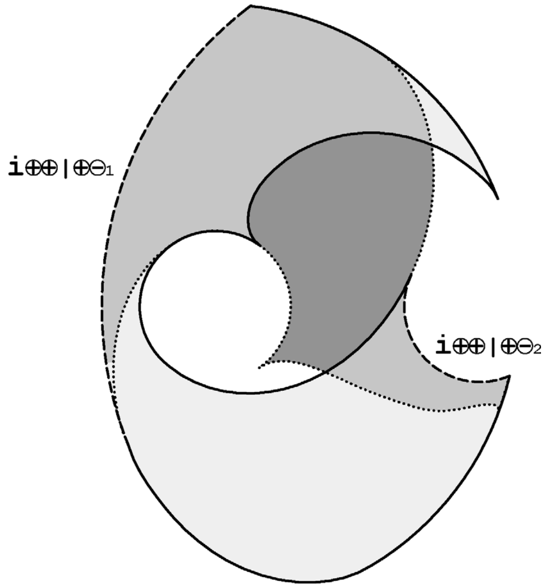

Fig. 12. ⊕ assembly mode regions for ⊕⊕ and ⊕⊖ working modes.

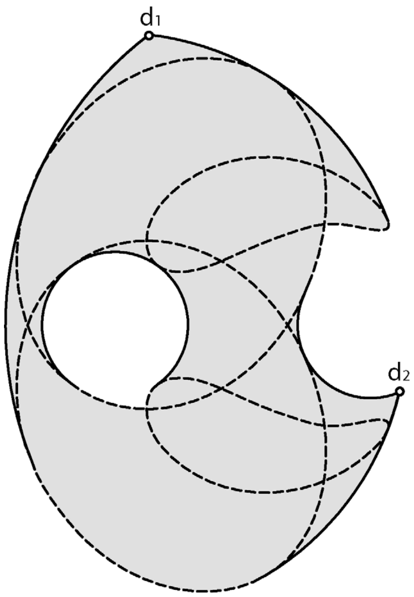

Fig. 13. Reachable workspace.

6. Reachable Workspace

All the regions represented in Fig. 10 correspond to the ⊕ assembly mode. All of them may be superimposed to obtain the total workspace representing all the positions the mechanism is able to reach with the same assembly mode. This practical workspace is shown in Fig. 13.

There are some special points d_i where two gates intersect, as shown in Fig. 13. Through these points, called double gates, it is possible to reach any of the four working modes.

Any position within this workspace may be reached without passing through a type II singularity. However, some considerations based on the previous concepts should be taken into account to make a path planning, since not all paths will be valid.

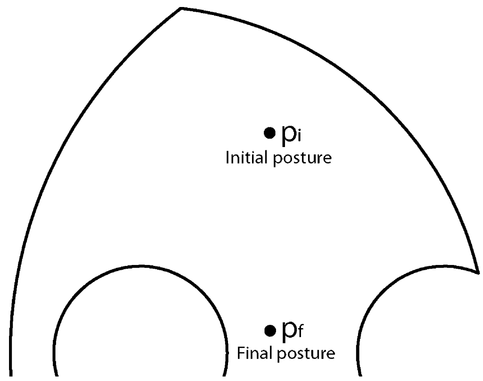

Fig. 14. Initial and final postures.

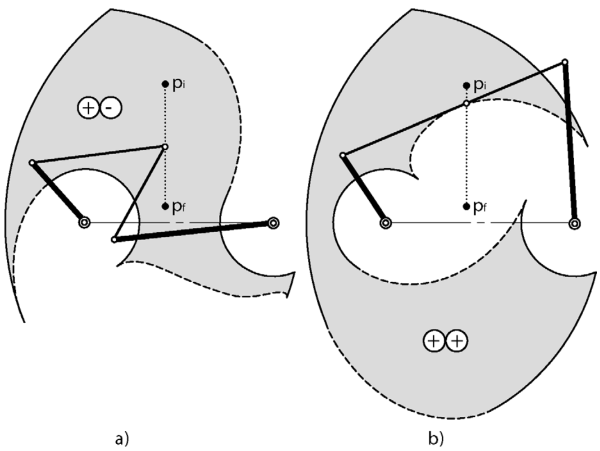

Fig. 15. Point-to-point motion planning in the $\oplus\ominus$ working mode and in the $\oplus\oplus$ working mode.

7. Point-to-Point Motion Planning

As an example let us consider the initial and final positions indicated in Fig. 14. Both points belong to the reachable workspace associated with the $\oplus$ assembly mode shown in Fig. 13. Hence, it is known that the mechanism is able to go from one to the other maintaining the same assembly mode at all times. In this section several examples concerning the point-to-point motion planning will be shown.

Firstly, it is necessary to determine which working modes are feasible for the initial and final positions, i.e., it is necessary to check which regions contain those positions inside them. The initial position is compatible with all working modes except $\ominus\ominus$, while the final position is only compatible with $\oplus\ominus$ and $\ominus\ominus$ working modes.

As the initial and final positions are in the same connected region corresponding to the $\oplus\ominus$ working mode, the most direct path would be to start from the initial position with the mechanism disposed in such working mode and go to the final position along a path completely contained in such region, as shown in Fig. 15(a).

However, if the mechanism in the initial position is assembled in the $\oplus\oplus$ working mode, a path completely contained in the starting region as the previous one is no longer possible, since the final position is no longer in the same region as the initial one and that path implies crossing a type II singularity, as shown in Fig. 15(b).

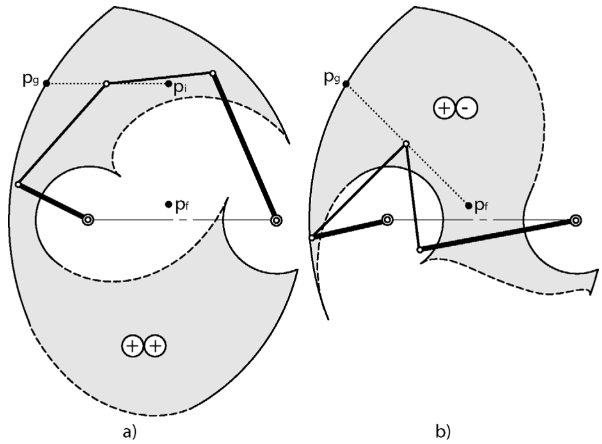

Fig. 16. Point to point motion planning starting in the $\oplus\oplus$ working mode and reaching the gate to pass to $\oplus\ominus$ working mode.

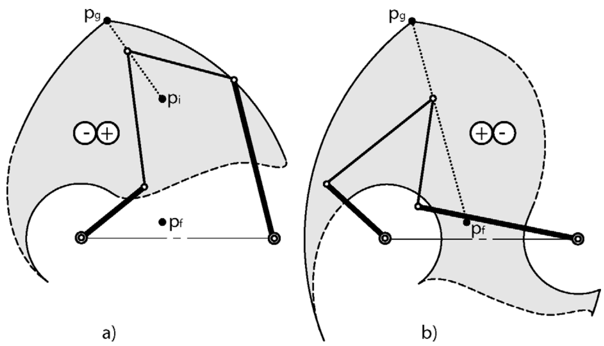

Fig. 17. Point-to-point motion planning starting in the $\ominus\oplus$ working mode and reaching the gate to pass to the $\oplus\ominus$ working mode.

Nevertheless, it has been seen that the final position is reachable in the $\oplus\ominus$ working mode and the gates allowing transition between both working modes are known. Thus, the path must pass through a gate position p_g, on one of these gate curves as shown in Fig. 16.

In Fig. 17 one of the double gate points, position p_g, is used to make a path planning starting at the $\ominus\oplus$ working mode and making a double working mode change by inverting both kinematic chains at the same time to reach the $\oplus\ominus$ working mode.

8. Joint Space

The previous sections were focussed on the workspace related to output variables x, y. In this section a study is carried out on the workspace and singularities from the input variables, θ_1, θ_2, viewpoint.

Type II singularity loci is given in the joint space by the equation

$$(L_2 \sin\theta_2 - L_1 \sin\theta_1)^2 + (d + L_2 \cos\theta_2 - L_1 \cos\theta_1)^2 = (l_1 \pm l_2)^2 \tag{11}$$

And type I singularity loci is given by

$$((L_1 + l_1)\sin\theta_1 - L_2 \sin\theta_2)^2 + ((L_1 + l_1)\cos\theta_1 - d - L_2 \cos\theta_2)^2 = l_2^2 \tag{12}$$

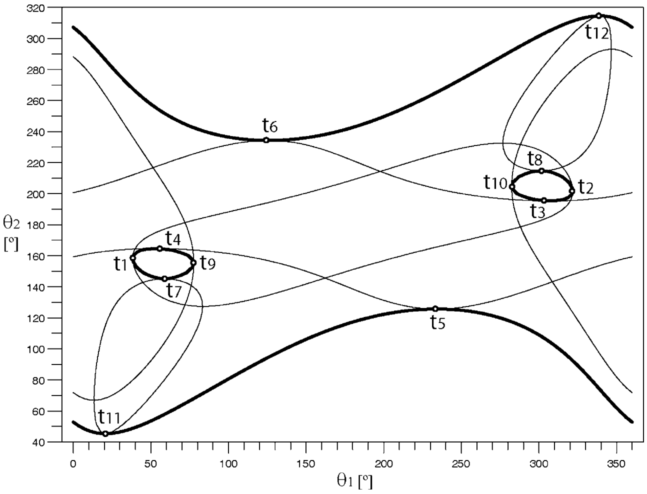

Fig. 18. Singularities in the joint space.

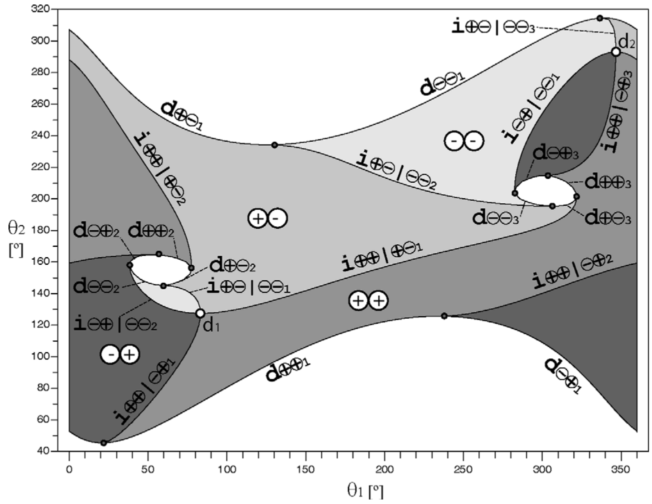

Fig. 19. Regions in the joint space in ⊕ assembly mode.

$$((L_1 - l_1)\sin\theta_1 - L_2\sin\theta_2)^2 + ((L_1 - l_1)\cos\theta_1 - d - L_2\cos\theta_2)^2 = l_2^2 \tag{13}$$

$$((L_2 + l_2)\sin\theta_2 - L_1\sin\theta_1)^2 + ((L_2 + l_2)\cos\theta_2 + d - L_1\cos\theta_1)^2 = l_1^2 \tag{14}$$

$$((L_2 - l_2)\sin\theta_2 - L_1\sin\theta_1)^2 + ((L_2 - l_2)\cos\theta_2 + d - L_1\cos\theta_1)^2 = l_1^2 \tag{15}$$

These curves are represented in Fig. 18, type II singularities with a thick line and type I singularities with a thin line. In this case type II singularities constitute the joint space boundaries, while type I singularities are inside the joint space. The same tangency cases occur between both singularity loci. In this case, the closed curves are generated by type I singularities and may be considered divided by those tangent points into several open curves. These open curves must be studied separately since a half of them constitute type I singularity positions for the mechanism in ⊕ assembly mode and the other half are solely associated with the mechanism type I singularities in ⊖ assembly mode. As in the previous sections, it will be assumed by way of example that the manipulator will work in ⊕ assembly mode. Then, only the type I singularities associated with such assembly mode, indicated in Fig. 19, will be considered. These type I singularity curves divide the input space into a series of adjacent regions corresponding to those obtained for the workspace and are also shown in Fig. 19.

The representation of the joint space implies a series of additional advantages. In this space it is possible to represent all the mechanism singularities associated with an assembly mode simultaneously, without having to divide into as many representations as the number of manipulator working modes. Furthermore, the path planning task is considerably simplified since in this space it can be immediately determined which is the gate which can enable the working mode change to make a motion from one position to another.

In addition, carrying out the point-to-point motion planning in this space enables better control on the real variation of the actuators, as shown in Fig. 20 related to the case set out in Fig. 16. In that case, the path planning executed in the workspace as straight paths $p_i p_{g1}$ and $p_{g1} p_f$ becomes curved lines in the joint space. On the contrary, p_i and p_f positions joined directly via a straight line in the joint space produce a linear variation in the actuators, but curved paths $p_i p_{g2}$ and $p_{g2} p_f$ in the workspace.

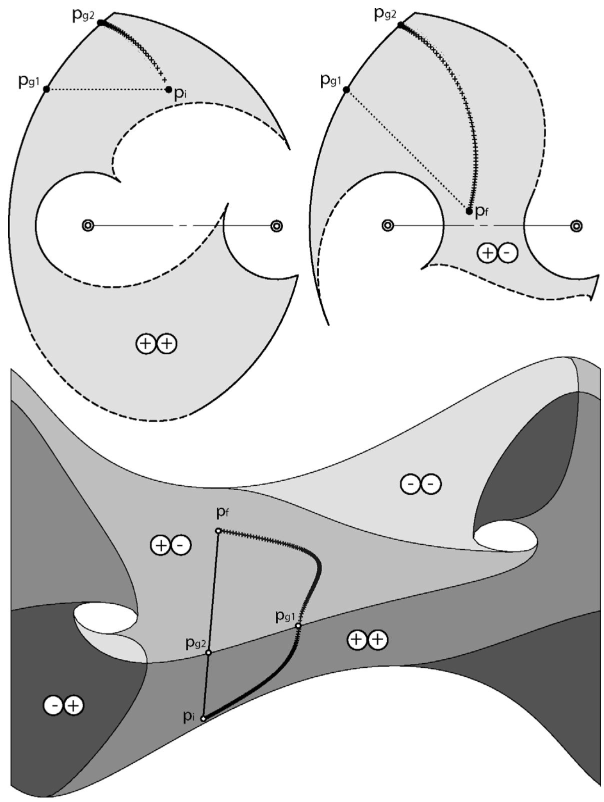

Fig. 20. Comparison between point to point motion planning in the workspace and in the joint space.

9. Path Planning

All these concepts can also be applied to perform the complete path planning. Obviously any desired path must be completely included in the reachable workspace. As an

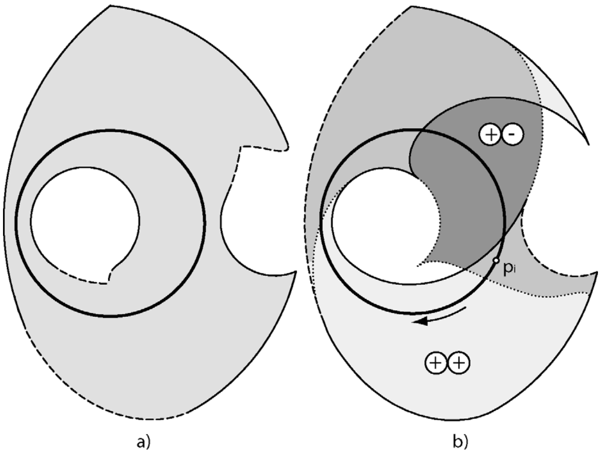

Fig. 21. Circular path in the reachable workspace.

example let us consider the circular path shown in Fig. 21(a). Firstly it is necessary to identify a set of regions, which overlapped completely contain the path. In this case, as shown in Fig. 21(b), two regions associated to the ⊕⊕ and ⊕⊖ working modes have been selected. As the path of this example is a closed curve, it is also necessary to choose a starting position, p_i, and a routing sense.

In this case the starting position is compatible with both chosen regions, so let us suppose for example that the manipulator is initially assembled in the ⊕⊕ working mode. As shown in Fig. 22 the path can evolve inside the ⊕⊕ region from the initial position p_i until the manipulator is close to cross a type II singularity curve. At a chosen distance from the singularity, position p_{m1}, the manipulator has to change the working mode in order to reach a new region to complete the path. Through gate position p_g the position p_{m2} is reached with the tool disconnected (p_{m1} and p_{m2} have the same coordinates in the workspace). From p_{m2} the path can evolve normally inside the ⊕⊖ region until the final position p_f.

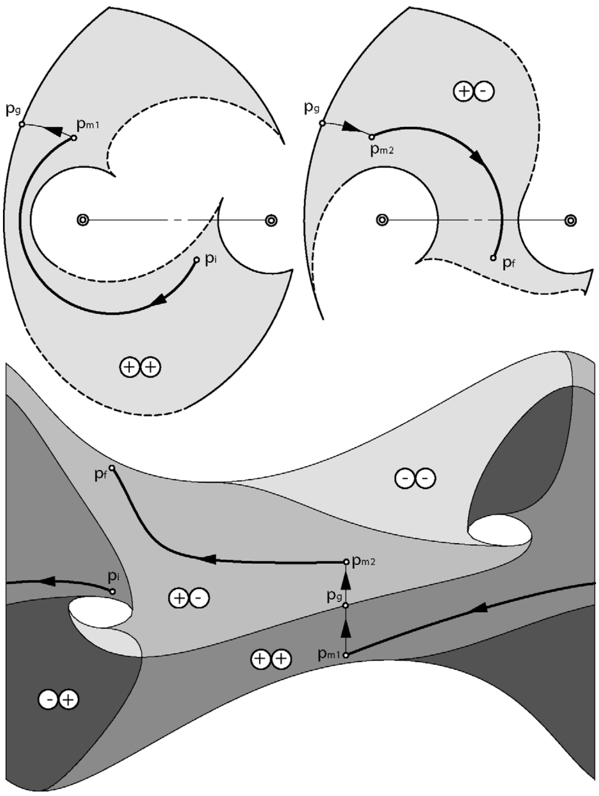

Fig. 22. Path planning starting in the ⊕⊕ working mode and reaching the gate to pass to ⊕⊖ working mode.

10. Systematisation

All the procedures shown in this paper have been applied to the 5R planar parallel manipulator. Nevertheless, these principles seem to be applicable to more complex platforms. The following general steps are provided:

1. Identify all working modes of the manipulator.
2. Make a singularity analysis. Obtain all type I and type II singular postures.
3. Distribute the type II singularities among the existing working modes.
4. Identify the n-dimensional regions associated to different assembly modes in each of the workspaces associated to the different working modes.
5. Superimpose all regions associated to the same assembly mode, from all working modes, in order to obtain the practical reachable workspace associated to that assembly mode.
6. Identify the gates, or type I singularities which connect the regions associated to the different working modes in that reachable workspace, to make the path planning.

11. Conclusions

From the concepts set out in this paper some conclusions can be achieved:

- Each working mode of the manipulator has different type II singularity curves.
- For each working mode a set of regions free from internal singularities can be found. These regions are delimited by two types of boundaries, the type I singularities and the type II singularities.
- For each working mode, type II singularities separate the different assembly modes and imply a loss of control. Therefore, such positions should always be avoided.
- On the contrary, type I singularities, despite not being suitable at operational level, do not imply a loss of control. Furthermore, it is possible to jump to other working modes by using them.
- Thus, it is possible to obtain all the regions associated with the same assembly mode, for each working mode, and perform the joining of all of them to obtain the manipulator reachable workspace for that assembly mode. A larger workspace is achieved enabling the mechanism to reach positions which would not have been possible if the mechanism would be forced to remain in the initial working mode at all times.
- To make an efficient path planning it is necessary to know which are the gates that allow passing from one region to another.

Acknowledgements

This research work was supported in part by the Spanish Ministerio de Ciencia y Tecnologia (Project DPI2005-02207), the FEDER funds of the European Union, the University of the Basque Country (Project GIU05/46) and the Grant (BFI104.148.R2) from the Basque Government.

References

1. J. P. Merlet, *Parallel robots* (Kluwer Academic Publishers, Norwell, MA, 2000).
2. C. M. Gosselin and J. Angeles, "Singularity analysis of closed loop kinematic chains," *IEEE Trans. Robot. Autom.* **6**(3), 281–290 (1990).
3. O. Altuzarra, C. Pinto, R. Aviles and A. Hernandez, "A practical procedure to analyze singular configurations in closed kinematic chains," *IEEE Trans. Robot.* **20**(6), 929–940 (2004).
4. D. Zlatanov, R. G. Fenton and B. Benhabib, "Singularity analysis of mechanisms and robots via velocity-equation model of the instantaneous kinematics," *ICRA* (2), 986–991 (1994).
5. J. P. Merlet, C. M. Gosselin and N. Mouly, "Workspace of planar parallel manipulators," *Mech. Mach. Theory* **33**(1–2), 7–20 (1998).
6. K. H. Hunt and E. J. F. "Primrose, Assembly configurations of some in-parallel-actuated manipulators," *Mech. Mach. Theory* **28**(1), 31–42 (1993).
7. J. MaaB, M. Kolbus, C. Budde, J. Hesselbach and W. Schumacher, "Control strategies for enlarging a spatial parallel robot's workspace by change of configuration," *Proceedings of the 5th Chemnitz Parallel Kinematics Seminar* (2006) 515–530.
8. C. Innocenti and V. Parenti-Castelli, "Singularity free evolution from one configuration to another in serial and fully parallel manipulators," *ASME J. Mech. Des.* **120**, 73–99 (1998).
9. D. Chablat and P. Wenger, "Workspace and assembly modes in fully parallel manipulators: A descriptive study," *Adv. Rob. kin: Anal. Control*, 117–126 (1998).
10. P. R. McAree and R. W. Daniel, An explanation of the never-spacial assembly changing motions for 3-3 parallel manipulators, *Int. J. Robot. Res.* **18**(6) 556–574 (1999).
11. D. C. Tao and A. S. Tall, "Analysis of a symmetrical five-bar linkage," *Prod. Engi.* **23**, 175–177 (1952).
12. G. Alici, "An inverse position analysis of five-bar planar parallel manipulators," *Robotica* **20**, 195–201 (2002).
13. G. Alici, "Determination of singularity contours for five-bar planar parallel manipulators," *Robotica* **18**, 569–575 (2000).
14. Theingi, C. Li, I. M. Chen and J. Angeles, "Singularity management of 2-DOF planar manipulator using coupled kinematics," *Int. Conf. Control, Autom. Robot. Vis.* (1), 402–407 (2002).
15. A. Bajpai and B. Roth, "Workspace and mobility of a closed-loop manipulator," *Int. J. Robot. Res.* **5**(2), 131–142 (1986).
16. D. Chablat, P. Wenger and J. Angeles, "The kinematic design of a 3-DOF hybrid manipulator," *Conf. Integr. Des. Manuf. Mech. Eng.* **2**(2), 385–392 (1998).
17. F. Gao, X. Zhang, Y. Zhao and H. Wang, "A physical model of the solution space and the atlas of the reachable workspace for 2-DOF parallel plane manipulators," *Mech. Mach. Theory* **31**(2), 173–184 (1996).
18. F. Gao, X. J. Liu and W. A. Gruver, "Performance evaluation of 2-DOF planar parallel robots," *Mech. Mach. Theory* **33**(6), 661–668 (1998).
19. X. J. Liu, J. Wang and G. Pritschow, "Kinematics, singularity and workspace of planar 5R symmetrical parallel mechanisms," *Mech. Mach. Theory* **41**(2), 145–169 (2006).
20. X. J. Liu, J. Wang and G. Pritschow, "Optimum design of the 5R symmetrical parallel manipulator with a surrounded and good-condition workspace," *Robot. Autom. Syst.* **54**(3), 221–233 (2006).
21. J. J. Cervantes-Sanchez, J. C. Hernandez-Rodriguez and J. G. Rendon-Sanchez, "On the workspace, assembly configurations and singularity curves of the RRRRR-type planar manipulator," *Mech. Mach. Theory* **35**(8), 1117–1139 (2000).
22. J. J. Cervantes-Sanchez, J. C. Hernandez-Rodriguez and J. Angeles, "On the kinematic design of the 5R planar symmetric manipulator," *Mech. Mach. Theory* **36**(11–12), 1301–1313 (2001).